

Systematics of parton fragmentation in e^+e^- and nuclear collisions

Thomas A. Trainor

CENPA 354290, University of Washington, Seattle, WA 98195, USA

(Received ?)

Parametrizations of fragmentation functions (FFs) from e^+e^- and $p\bar{p}$ collisions are combined with a parton spectrum model in a pQCD folding integral to produce minimum-bias *fragment distributions*. A model of in-medium FF modification is included. Calculated fragment distributions are compared with *hard components* from p-p and Au-Au p_t spectra. Data are well described by pQCD over a large kinematic region for a range of Au-Au centralities.

PACS numbers: 12.38.Qk, 13.87.Fh, 25.75.Ag, 25.75.Bh, 25.75.Ld, 25.75.Nq

Keywords: fragmentation, jet quenching, pQCD, heavy ion collisions, two-component model

I. INTRODUCTION

RHIC collisions are conventionally described in terms of hydrodynamic (hydro) evolution of a thermalized bulk medium and energy loss of energetic partons (hard probes) in that medium. Hydro should dominate p_t spectra below 2 GeV/c, parton fragmentation above 5 GeV/c, and “quark coalescence” in the intermediate p_t interval.

However, recent analysis of spectrum and correlation structure has revealed *minijet* structures in RHIC collisions [1, 2, 3, 4, 5, 6, 7]. Two-component analysis of p-p and Au-Au spectra reveals a corresponding *hard component* (minimum-bias *fragment distribution*), suggesting that jet phenomena extend down to 0.1 GeV/c [8, 9]. Minijets [10] appear to dominate the transverse dynamics of nuclear collisions at energies above $\sqrt{s_{NN}} \sim 15$ GeV and provide unbiased access to fragment distribution structure down to a small cutoff energy for scattered partons (3 GeV) and to the smallest detectable fragment momenta (~ 0.1 GeV/c).

Minijets can be studied in the form of p_t -spectrum hard components isolated via the two-component spectrum model. Measured hard components are compared with pQCD fragment distributions (FDs). Parton spectrum parameters and modifications to fragmentation functions (FFs) in more-central Au-Au collisions are inferred [11]. The goal is a comprehensive pQCD description of all nuclear collisions.

II. TWO-COMPONENT MODEL

The two-component (soft+hard) spectrum model was first obtained from a Taylor-series expansion of p-p p_t spectra on uncorrected event multiplicity \hat{n}_{ch} for ten multiplicity classes [8]. The soft component was interpreted as longitudinal nucleon fragmentation, the hard component as transverse scattered-parton fragmentation.

The two-component model for p-p collisions with soft and hard multiplicities $n_s + n_h = n_{ch}$ is

$$\frac{1}{n_s(\hat{n}_{ch})} \frac{1}{y_t} \frac{dn_{ch}(\hat{n}_{ch})}{dy_t} = S_0(y_t) + \frac{n_h(\hat{n}_{ch})}{n_s(\hat{n}_{ch})} H_0(y_t) \quad (1)$$

Coefficient n_h/n_s scales as $\alpha \hat{n}_{ch}$, $S_0(y_t)$ is a Lévy distribution on m_t and $H_0(y_t)$ is a Gaussian plus QCD power-law tail on transverse rapidity $y_t = \ln\{(m_t + p_t)/m_0\}$ [8]. To compare with A-A spectra we define $S_{pp} = (1/y_t) dn_s/dy_t$ with reference model $n_s S_0$ and similarly for $H_{pp} \leftrightarrow n_h H_0$.

The corresponding two-component model for per-participant-pair A-A spectra is

$$\begin{aligned} \frac{2}{n_{part}} \frac{1}{y_t} \frac{dn_{ch}}{dy_t} &= S_{NN}(y_t) + \nu H_{AA}(y_t; \nu) \quad (2) \\ &= S_{NN}(y_t) + \nu r_{AA}(y_t; \nu) H_{NN}(y_t), \end{aligned}$$

where S_{NN} ($\sim S_{pp}$) is the soft component and H_{AA} is the A-A hard component (with reference $H_{NN} \sim H_{pp}$) [8, 9]. Ratio $r_{AA} = H_{AA}/H_{NN}$ is an alternative to nuclear modification factor R_{AA} . Centrality measure $\nu \equiv 2n_{binary}/n_{participant}$ estimates the mean nucleon path length. We are interested in the evolution of hard component H_{AA} or ratio r_{AA} with A-A centrality.

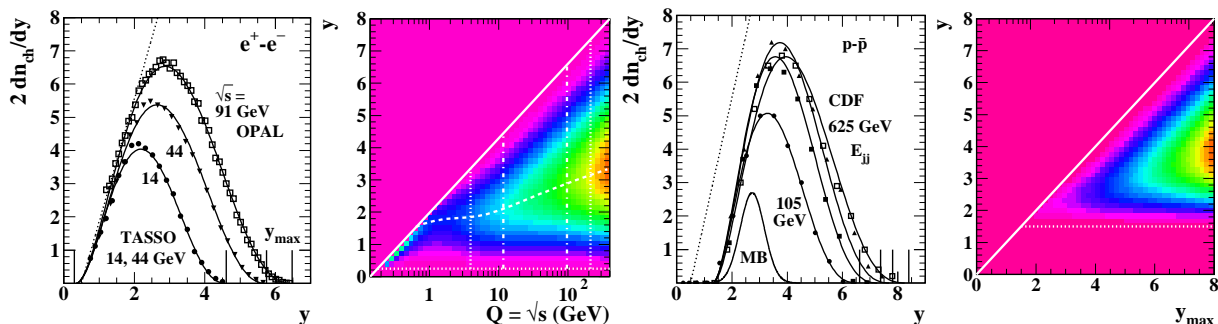


FIG. 1: First: Fragmentation functions (FFs) from e^+e^- collisions for three energies with β -distribution parametrizations (solid curves), Second: Full e^+e^- FF parametrization on parton rapidity y_{max} , Third: FFs from p- \bar{p} collisions for several dijet energies, Fourth: Full p- \bar{p} FF parameterization on parton rapidity.

III. FRAGMENTATION FUNCTIONS

e^+e^- (e-e) fragmentation functions (FFs) have been parametrized accurately over the full kinematic region relevant to nuclear collisions [12]. Light-quark and gluon fragmentation functions $D_{xx}(x, Q^2) \leftrightarrow D_{xx}(y, y_{max})$ ($xx = e-e, p-p, A-A$) are described above energy scale $Q = 2E_{jet} \sim 10$ GeV by a two-parameter *beta distribution* $\beta(u; p, q)$ on normalized rapidity u [12]. Fragment rapidity for unidentified hadrons is $y = \ln[(E + p)/m_\pi]$, and parton rapidity $y_{max} = \ln(Q/m_\pi)$. Parameters (p, q) vary slowly and linearly with y_{max} above $Q = 10$ GeV and can be extrapolated down to $Q \sim 4$ GeV.

Fig. 1 (first panel) shows measured FFs for three energy scales from HERA/LEP [13, 14]. The curves are $\beta(p, q)$ parametrizations which describe data over the entire fragment momentum range. Fig. 1 (second panel) shows the FF ensemble vs energy scale Q as a surface plot [12].

Figure 1 (third panel) shows FF data from p- \bar{p} collisions at FNAL [15]. The dotted line represents the lower limit for e-e FFs. There is a significant systematic difference between p-p and e-e FFs. The CDF FFs also reveal suppression at larger parton energies relative to LEP e-e systematics. Fig. 1 (fourth panel) is a surface plot of the p-p FF parametrization [11]—the e-e FF parametrization modified by cutoff factor

$$g_{cut}(y) = \tanh\{(y - y_0)/\xi_y\} \quad y > y_0, \quad (3)$$

with $y_0 \sim \xi_y \sim 1.5$ determined by the CDF FF data [15]. The cutoff represents real fragment and energy loss from p-p relative to e-e FFs. The

difference suggests that FFs may not be universal.

IV. pQCD FRAGMENT DISTRIBUTIONS

The parton p_t spectrum from minimum-bias scattering into an η acceptance near projectile mid-rapidity can be parametrized as

$$\begin{aligned} \frac{1}{p_t} \frac{d\sigma_{dijet}}{dp_t} &= f_{cut}(p_t) \frac{A_{p_t}}{p_t^{n_{QCD}}} \rightarrow \frac{d\sigma_{dijet}}{dy_{max}} \quad (4) \\ &= f_{cut}(y_{max}) A_{y_{max}} \exp\{-(n_{QCD} - 2)y_{max}\}, \end{aligned}$$

with $y_{max} \equiv \ln(2p_t/m_\pi)$. The cutoff factor

$$f_{cut}(y_{max}) = \{\tanh[(y_{max} - y_{cut})/\xi_{cut}] + 1\}/2 \quad (5)$$

represents the minimum parton momentum which can lead to detectable charged hadrons as neutral pairs. Parton spectrum and cutoff parameters are determined by comparing FDs with p-p and Au-Au spectrum hard components.

Fig. 2 (first panel) shows the parton spectrum (solid curve) with cutoff ~ 3 GeV inferred from a p-p p_t spectrum hard component [11]. The bold dotted curve is an ab-initio pQCD calculation [16]. The spectrum integrates to 2.5 ± 0.6 mb, consistent with pQCD theory [17].

The pQCD folding (convolution) integral used to obtain fragment distributions is

$$\frac{d^2n_h}{dy d\eta} \approx \frac{\epsilon(\delta\eta, \Delta\eta)}{\sigma_{NSD} \Delta\eta} \int_0^\infty dy_{max} D(y, y_{max}) \frac{d\sigma_{dijet}}{dy_{max}}, \quad (6)$$

where $D(y, y_{max})$ is the FF ensemble from some collision system (e-e, p-p, A-A, in-medium or in-vacuum), and $d\sigma_{dijet}/dy_{max}$ is the parton spectrum [11]. Hadron spectrum hard component

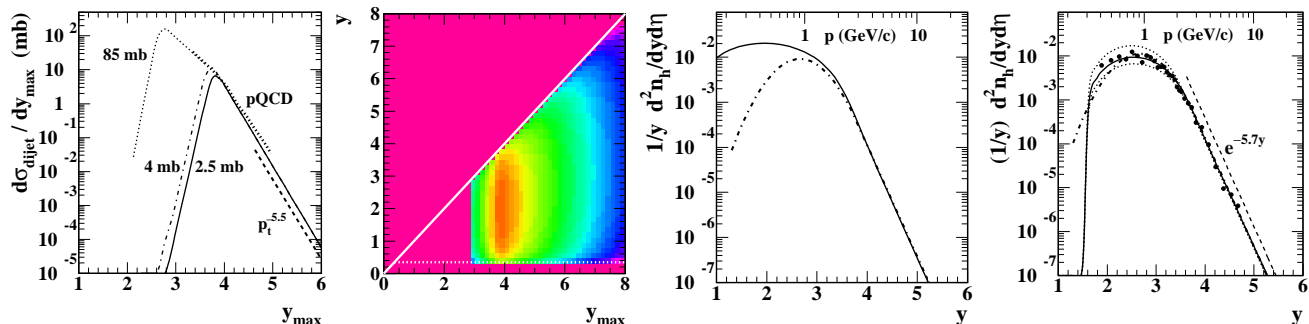


FIG. 2: First: Parton spectra inferred from this analysis for p-p collisions (solid curve) and central Au-Au collisions (dash-dotted curve) compared to an ab-initio pQCD theory result (bold dotted curve [16]), Second: pQCD folding-integral argument for e^+e^- FFs, Third: e-e FD (solid curve) and p-p hard-component reference (dash-dotted curve), Fourth: Fragment distribution (solid curve) compared to p-p hard-component data (points). Dotted curves correspond to $\pm 10\%$ change in parton spectrum cutoff energy about 3 GeV.

$d^2 n_h / dy d\eta$ represents the fragment yield from scattered parton pairs into η acceptance $\delta\eta$. Efficiency factor $\epsilon \sim 0.5$ includes the probability that the second jet also falls within $\delta\eta$. $\Delta\eta \sim 5$ is the effective 4π η interval for scattered partons. σ_{NSD} (~ 36 mb for $\sqrt{s_{NN}} = 200$ GeV) is the cross section for NSD p-p collisions.

Fig. 2 (second panel) shows integrand $D_{ee}(y, y_{\text{max}}) \frac{d\sigma_{\text{dijet}}}{dy_{\text{max}}}$ of Eq. (6) with unmodified FFs from e-e collisions and lower bound at $y_{\text{min}} \sim 0.35$ ($p_t \sim 0.05$ GeV/c) (dotted line). Fig. 2 (third panel) shows the corresponding FD (solid curve), the “correct” FD describing inclusive hadrons from partons produced by *free* parton scattering from p-p collisions. The dash-dotted curve is the hard-component model inferred from p-p spectrum data [8]. The FD from e-e FFs lies well above the measured p-p hard component for hadron $p < 2$ GeV/c ($y < 3.3$), and the mode is shifted down to ~ 0.5 GeV/c. The “correct” e-e FD strongly disagrees with the hard component of the p-p p_t spectrum. Nevertheless, the e-e FD is the proper reference for nuclear collisions [11].

Fig. 2 (fourth panel) shows FD $H_{NN-\text{vac}}$ as the solid curve, with measured FFs from p-p collisions. The mode of the FD is ~ 1 GeV/c. The solid points are hard-component data from p-p collisions and the dash-dotted curve is p-p model function H_{pp} [8]. The comparison determines parton spectrum parameters $y_{\text{cut}} = 3.75$ ($E_{\text{cut}} \sim 3$ GeV), $A_{y_{\text{max}}}$ and exponent $n_{QCD} = 7.5$ and establishes a quantitative relationship among parton spectrum, measured FFs and measured spec-

trum hard components over all p_t , not just a restricted interval above 2 GeV/c.

V. PARTON “ENERGY LOSS” MODEL

Fragmentation in A-A collisions requires a model of parton “energy loss” or medium modification. We adopt a minimal model of FF modification (Borghini-Wiedemann or BW) [18]. Figure 3 (first panel) illustrates the BW model (cf. Fig. 1 of [18], $\xi_p = \ln(p_{\text{jet}}/p) = \ln(2p_{\text{jet}}/m_\pi) - \ln(2p/m_\pi) \sim y_{\text{max}} - y$). In-vacuum e-e FFs for $Q = 14$ and 200 GeV from the beta parametrization are shown as dashed and solid curves [12]. We can simulate BW accurately by changing parameter q in $\beta(u; p, q)$ by $\Delta q \sim 1$ (dash-dotted and dotted curves) [11]. Small reductions at larger fragment momenta (smaller ξ_p) are compensated by much larger increases at smaller momenta. The largest changes (central Au-Au) correspond to an inferred 25% leading-parton fractional “energy loss.” Fig. 3 (second panel) shows the modified e-e FF ensemble with FF modes shifted to smaller fragment rapidities y .

Figure 3 (third panel) shows $H_{ee-\text{med}}$ (solid curve), the FD obtained by inserting in-medium e-e FFs from the second panel into Eq. (6). The dotted curve is the $H_{ee-\text{vac}}$ reference from in-vacuum e-e FFs. The mode of $H_{ee-\text{med}}$ is ~ 0.3 GeV/c. Fig. 3 (fourth panel) shows results for p-p FFs. Major differences between p-p and e-e FDs appear below $p_t \sim 2$ GeV/c ($y_t \sim 3.3$). Conventional comparisons with theory (e.g., data

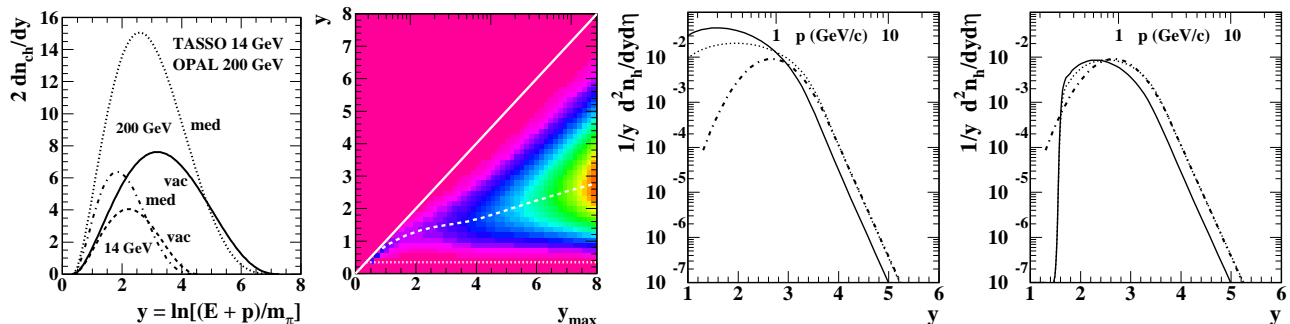


FIG. 3: First: e^+e^- FFs for two energies unmodified (solid and dashed curves) and modified to emulate parton “energy loss” [18] (dash-dotted and dotted curves), Second: e^+e^- FF ensemble modified according to [18], Third: Medium-modified FD from e^+e^- FFs (solid curve) compared to in-vacuum e^+e^- FD (dotted curve) Fourth: Medium-modified FD from p- \bar{p} FFs (solid curve) compared to in-vacuum N-N FD (dotted curve).

vs NLO FDs) typically do not extend below 2 GeV/c [19]. The large difference between the two collision systems below 2 GeV/c reveals that the small- p_t region, conventionally assigned to hydro phenomena, may be essential for effective study of fragmentation evolution in A-A collisions.

VI. FRAGMENTATION EVOLUTION

Measured FFs are combined with a parametrized pQCD parton spectrum to produce calculated FD_{xx} for comparison with measured spectrum hard components H_{xx} . Figure 4 (first panel) shows spectrum hard components H_{AA} (solid curves) for five centralities from 200 GeV Au-Au collisions [9]. The hard components scale proportional to n_{binary} , as expected for parton scattering and fragmentation (jets). The points are from 200 GeV NSD p-p collisions [8]. The dashed curve is H_{NN-vac} , and the upper dotted curve is H_{ee-med} with $\Delta q = 1.15$, which corresponds to the most-central Au-Au curve (0-12%). The parton spectrum cutoff for H_{ee-med} has been reduced from 3 GeV ($y_{max} = 3.75$) to 2.7 GeV ($y_{max} = 3.65$) to match the central Au-Au hard component near $y_t = 3$.

Jet-related spectrum structure can also be studied with ratios. The conventional spectrum ratio at RHIC is R_{AA} . Because it includes the spectrum soft component R_{AA} strongly suppresses fragment contributions at smaller y_t . Hard-component evolution with centrality is better resolved by ratio $r_{AA} \equiv H_{AA}/H_{NN}$. However, studies in Ref. [11] reveal that the proper refer-

ence for all systems is the in-vacuum FD from e-e FFs, not p-p FFs. We therefore define ratios $r_{xx} = FD_{xx-yyy}/FD_{ee-vac}$ with $xx = ee, NN, AA$ and $yyy = med$ or vac to be compared with equivalent spectrum hard components H_{xx-yyy} .

Figure 4 (second panel) shows ratios redefined in terms of the ee-vac reference: H_{pp} (p-p data – points), H_{AA} (peripheral Au-Au data – solid curve [9]) and calculated H_{ee-med} (dash-dotted curve) and H_{NN-vac} (dashed curve) all divided by reference H_{ee-vac} . Strong suppression of p-p and peripheral Au-Au data apparent at smaller y_t results from the cutoff of p-p FFs.

Figure 4 (third panel) shows measured H_{AA}/H_{ee-vac} for more-central Au-Au collisions (solid curves) above a transition point on centrality at $\nu \sim 2.5$, with partial restoration of the suppressed region at smaller y_t and strong suppression at larger y_t . The latter has been a major observation at RHIC (high- p_t suppression, “jet quenching” [20]). Newly apparent is the accompanying large *increase* in fragment yield *below* 2 GeV/c, still strongly correlated with the parent parton [7]. Changes in fragmentation depend strongly on centrality near the transition point. It is remarkable that the trend at 10 GeV/c corresponds closely to the trend at 0.5 GeV/c. H_{pp} , H_{AA} and ratios based on the e-e in-vacuum reference are well described by pQCD FDs from 0.3 to 10 GeV/c [11].

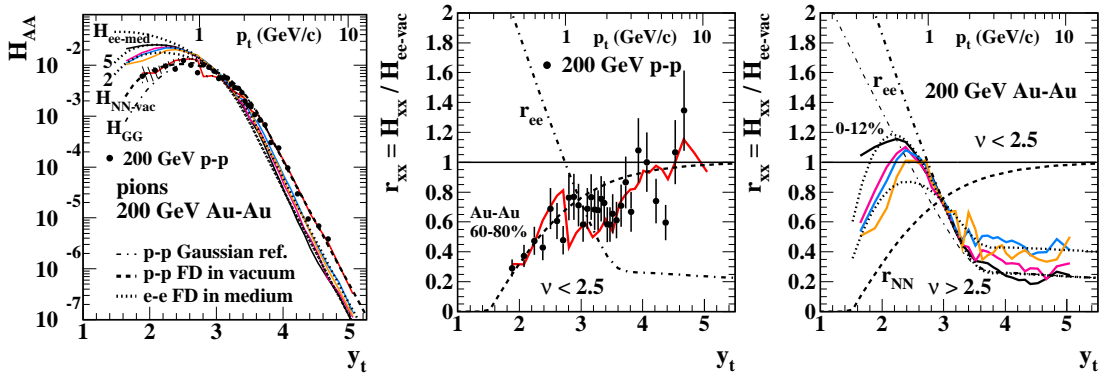


FIG. 4: First: Hard-component evolution in central Au-Au collisions vs centrality [9]. Large increases at smaller y_t accompany suppression at larger y_t . Second: FD ratios relative to an ee-vacuum reference for Au-Au collisions below the sharp transition, Third: FD ratios above the sharp transition revealing major changes in FD structure,

VII. CONCLUSIONS

Hard components of p_t spectra can be identified with minimum-bias parton fragmentation in nuclear collisions. Minimum-bias fragment distributions (FDs) can be calculated by folding a power-law parton energy spectrum with parametrized fragmentation functions (FFs) derived from e^+e^- and $p\bar{p}$ collisions. Alterations to FFs due to parton “energy loss” or “medium modification” in Au-Au collisions are modeled by adjusting FF parametrizations consistent with rescaling QCD splitting functions. The reference

for all nuclear collisions is the FD derived from in-vacuum e^+e^- FFs. Relative to that reference the hard component for p-p and peripheral Au-Au collisions is found to be *strongly suppressed* for smaller fragment momenta. At a specific point on centrality the Au-Au hard component transitions to enhancement at smaller momenta and suppression at larger momenta, consistent with FDs derived from medium-modified e^+e^- FFs.

I thank the organizers of ISMD 2009 for a delightful and informative conference. This work was supported in part by the Office of Science of the US DOE under grant DE-FG03-97ER41020.

-
- [1] R. J. Porter and T. A. Trainor (STAR Collaboration), J. Phys. Conf. Ser. **27**, 98 (2005), hep-ph/0506172.
 - [2] R. J. Porter and T. A. Trainor (STAR Collaboration), PoS C **FRNC2006**, 004 (2006).
 - [3] J. Adams *et al.* (STAR Collaboration), Phys. Rev. C **73**, 064907 (2006).
 - [4] Q. J. Liu, D. J. Prindle and T. A. Trainor, Phys. Lett. B **632**, 197 (2006).
 - [5] J. Adams *et al.* (STAR Collaboration), J. Phys. G: Nucl. Part. Phys. **32**, L37 (2006).
 - [6] J. Adams *et al.* (STAR Collaboration), J. Phys. G **33**, 451 (2007).
 - [7] M. Daugherty (STAR Collaboration), J. Phys. G **35**, 104090 (2008).
 - [8] J. Adams *et al.* (STAR Collaboration), Phys. Rev. D **74**, 032006 (2006).
 - [9] T. A. Trainor, Int. J. Mod. Phys. E **17**, 1499 (2008), arXiv:0710.4504.
 - [10] X. N. Wang, Phys. Rev. D **46**, R1900 (1992).
 - [11] T. A. Trainor, Phys. Rev. C **80**, 044901 (2009), arXiv:0901.3387.
 - [12] T. A. Trainor and D. T. Kettler, Phys. Rev. D **74**, 034012 (2006).
 - [13] W. Braunschweig *et al.* (TASSO Collaboration), Z. Phys. C **47**, 187 (1990).
 - [14] M. Z. Akrawy *et al.* (OPAL Collaboration) Phys. Lett. B, **247**, 617 (1990).
 - [15] K. Goulianos (CDF Collaboration), Proceedings of the “QCD and high energy hadronic interactions,” XXXII Rencontres de Moriond, Les Arces, France, March 22-29, 1997,
 - [16] F. Cooper, E. Mottola and G. C. Nayak, Phys. Lett. B **555**, 181 (2003).
 - [17] I. Sarcevic, S. D. Ellis and P. Carruthers, Phys. Rev. D **40**, 1446 (1989).
 - [18] N. Borghini and U. A. Wiedemann, hep-ph/0506218.
 - [19] A. Adare *et al.* (PHENIX Collaboration), Phys. Rev. D **76**, 051106 (2007).

- [20] C. Adler *et al.* (STAR Collaboration), Phys. Rev. Lett. **89**, 202301 (2002).